Temperature distribution in port wine stain following pulsed irradiation by a dual-wavelength Nd:YAG laser

Boris Majaron[*a,b], Bernard Choi[b], J. Stuart Nelson[b,c]

[a]Jožef Stefan Institute, Ljubljana, Slovenia
[b]Beckman Laser Institute and Medical Clinic, University of California at Irvine
[c]Department of Biomedical Engineering, University of California at Irvine

ABSTRACT

In therapy of port wine stain (PWS) birthmarks using pulsed green or yellow lasers, non-specific absorption by epidermal melanin reduces the amount of incident radiation that reaches the target PWS blood vessels. The related epidermal heating can induce blistering, dyspigmentation, or scarring, which limits the applicable radiant exposure, thus adversely affecting the efficacy of treatment in many patients. Our objective was to assess temperature depth profiles induced in PWS skin by a novel Nd:YAG laser emitting simultaneously at 1064 and 532 nm. The results should help determine safe radiant exposures for use in future clinical trials. The underlying hypothesis is that the added 1064 nm radiation may lead to a higher temperature increase in PWS relative to the epidermis, in comparison with a customary KTP/Nd:YAG laser system for vascular treatments (emitting at 532 nm only). The laser induced temperature profiles were determined in vivo using pulsed photothermal radiometry. A PWS test site was irradiated with a sub-therapeutic laser pulse and the transient change of the infrared radiant emission was recorded by a fast infrared camera. The laser-induced temperature profiles were reconstructed by solving the thermal-radiative inverse problem using an iterative minimization algorithm.

Keywords: depth profiling, dermatologic laser surgery, dual-wavelength laser, pulsed photothermal radiometry, vascular lesions.

1. INTRODUCTION

Port wine stain birthmarks (PWS) consist of a normal epidermis overlying an abnormal plexus of dilated blood vessels within the most superficial millimeter of the dermis. Depth distribution of PWS blood vessels varies from patient to patient, with the highest fractional blood content on average 0.2–0.4 mm below the epidermal-dermal junction.[1] Since most of the PWS lesions occur on the face, they represent a clinically significant problem with potentially devastating psychological and physical complications.

PWS therapy currently utilizes selective photocoagulation of the ectatic vasculature using pulsed green or yellow lasers. However, non-specific absorption by epidermal melanin reduces the amount of incident radiation that reaches the subsurface target chromophores - hemoglobin in PWS blood vessels. Moreover, excessive epidermal heating can induce blistering, dyspigmentation, or scarring of skin. Despite the recent implementation of dynamic cooling of human skin,[2,3] this effect limits the radiant exposure that can be safely applied in therapy, thereby adversely affecting treatment efficacy in many patients.

[*] Dr. Boris Majaron, Jožef Stefan Institute, Jamova 39, SI–1000 Ljubljana, Slovenia; http://www.ijs.si/ijs.html; boris.majaron@ijs.si, majaron@laser.bli.uci.edu; phone: +386 1 477-3208, fax: +386 1 423-5400, 425-1077.

The main objective of present study was to measure temperature depth profiles induced in PWS skin in vivo by a novel laser system, emitting simultaneously at 1064 nm and 532 nm. The results, when compared with those obtained by using a customary KTP/Nd:YAG laser for vascular treatments (emitting at 532 nm only) should enable determination of safe radiant exposures for use in clinical trials of the novel laser system. Because the melanin absorption decreases with increasing wavelength,[4] the hypothesis is that the additional irradiation at 1064 nm may induce a higher temperature rise in the PWS relative to the epidermis, as compared to irradiation at 532 nm alone. Moreover, recent evidence indicates safe and successful applications of near infrared (IR) lasers in therapy of vascular lesions, despite the absence of spatial selectivity in absorption of near IR radiation.[5,6,7]

The laser-induced temperature distribution were measured by means of pulsed photothermal radiometry (PPTR). PPTR is based on time-resolved acquisition of infrared (IR) emission from the sample surface after pulsed laser exposure. With known optical and thermal properties of the sample, the temperature depth profiles can be reconstructed from acquired transient radiometric signals by solving the inverse problem of heat diffusion and blackbody emission.[8,9] Such an approach is very suitable for depth profiling of optically scattering samples, including biological tissues,[10,11,12,13] and has been suggested earlier for characterization of PWS lesions.[14,15,16] Moreover, by recording radiative emission from the skin surface with high lateral resolution, three-dimensional imaging of in vivo vasculature has been demonstrated.[17,18,19] In the present work, we apply PPTR to compare the effect of two different laser systems on the same PWS site, aiming at assessing the clinically applicable light dosages and subsequent therapeutic effect of a novel laser system.

2. METHODOLOGY

2.1 Lasers and PWS site preparation

The Tandem laser system prototype (provided by Fotona, Ljubljana, Slovenia) emits 1–50 ms long pulses at wavelengths of 532 and 1064 nm simultaneously. Approximately 36% of the total pulse energy is emitted at 532 nm, the remaining 64% at 1064 nm. The system has obtained 510k approval from the US Food and Drugs Administration (FDA) for treatment of vascular lesions. For the purposes of PPTR measurements, 1 ms pulses were used; the radiant exposure at the skin surface was very low, $H_0 = 0.31$ J/cm^2. For comparison measurements, we used a standard KTP/Nd:YAG dermatologic laser system emitting at 532 nm (VersaPulse by Lumenis, Santa Clara, CA), at 2 ms pulse duration. The radiant exposure at the skin surface was also sub-therapeutic: $H_0 = 1.81$ J/cm^2.

The stated radiant exposure values were determined by measuring the pulse energy transmitted through a 0.72 mm diameter pinhole in the object plane. The pyroelectric detector (J25LP-1, Molectron, Portland, OR) was customized and re-calibrated to allow measurements of such relatively long laser pulses. Homogeneity of the irradiation was verified by laterally scanning the aperture within the field of view of the infrared camera.

(a) (b)

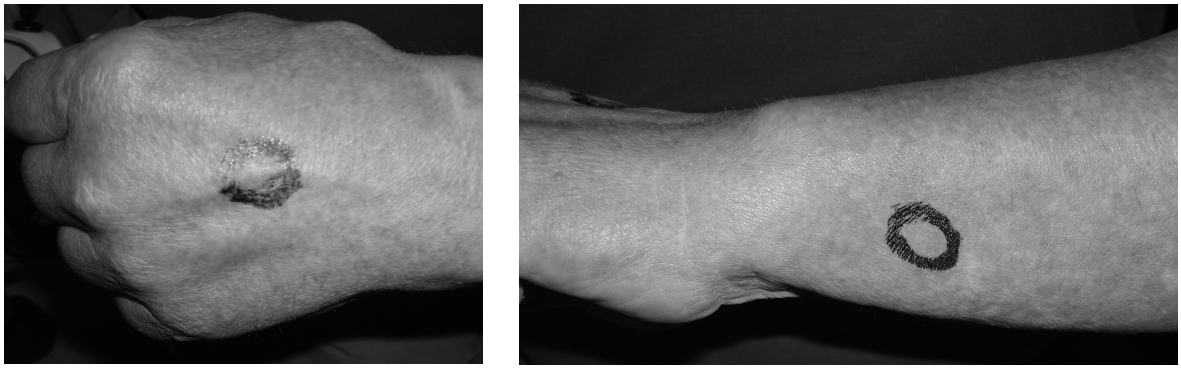

Figure 1: PWS test sites on volunteer patient's skin: (a) - site A, on the hand; (b) - site B, on the forearm.

Two PWS sites on the hand and forearm (Figs. 1a and 1b, respectively) of a volunteer patient were irradiated in the PPTR measurements. Prior to irradiation, the selected areas were shaved, and stratum corneum removed by tape stripping. The remnants of stratum corneum and glue were subsequently wiped away with ethanol. After re-moistening the skin with saline pads and wiping off excess liquid with paper tissue, the prepared site was positioned in the 1 cm aperture of the PPTR setup (see Fig. 2).

2.2 Pulsed photothermal radiometry – basics

Detailed discussion of PPTR depth profiling in semi-infinite media can be found elsewhere.[15,20] In short, one-dimensional approximation is valid as long as the laser irradiated spot (>5 mm in diameter in our experiments) is much larger than the involved optical penetration depths and thermal diffusion lengths. Planck's law of radiation, which describes the locally emitted power density at wavelength λ, is linearized around the initial skin temperature, T_0: $B_\lambda(T) \approx B_\lambda(T_0) + B_\lambda'(T_0)\,\Delta T$. Due to the finite absorption coefficient of emitted IR radiation (μ_{IR}), radiometric signal from a non-uniformly heated object is composed of appropriately attenuated contributions from different depths z. The radiometric signal $S_\lambda(t)$ is thus expressed as

$$S_\lambda(t) \;=\; C\,B_\lambda(T_0) \;+\; C\,B_\lambda'(T_0)\,\mu_{IR}\int_{z=0}^{\infty}\Delta T(z,t)\,e^{-\mu_{IR}z}\,dz\,, \qquad (1)$$

where constant C accounts for optical properties of the sample surface and collection optics, and detector specifics. Temperature field evolution in the sample, $\Delta T(z,t)$, is a convolution of the laser-induced temperature rise, $\Delta T(z,t=0)$, and the thermal point-spread function of the sample. Since the latter is known explicitly,[15] convolution with the exponential attenuation function in (1) can be performed, yielding a simple integral expression for the transient part of the radiometric signal, $\Delta S_\lambda(t)$:

$$\Delta S_\lambda(t) = \int_{z=0}^{\infty} K(z,t)\,\Delta T(z,0)\,dz\,. \qquad (2)$$

In the following, we apply kernel function $K(z,t)$ as derived by Milner *et al.*[15] (with thermal diffusivity of skin $D = 1.1 \times 10^{-7}$ m^{2}s^{-1}, and the reduced heat transfer coefficient at the surface of $h = 0.02$ m^{-1}).

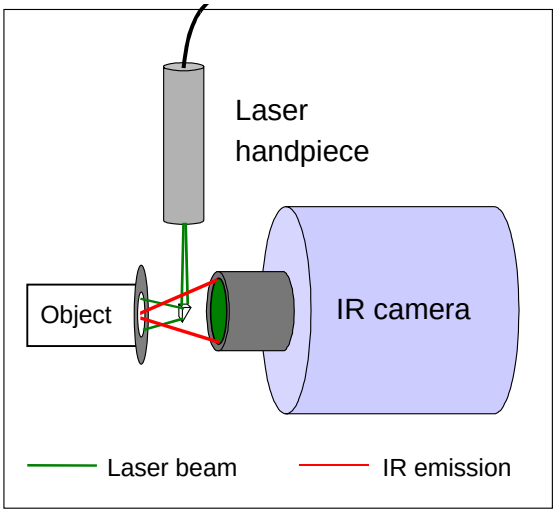

Figure 2: Schematic diagram of the pulsed photothermal radiometry (PPTR) setup. Light emitted from the laser handpiece is directed onto the sample surface by a microprism. A fixed 1 cm aperture enables accurate focusing of the IR camera imaging optics.

2.3 Experimental setup, signal acquisition, and data analysis

A schematic diagram of the PPTR experimental setup is presented in Figure 2. Light pulse emitted from the laser handpiece is reflected by onto PWS skin site by a micro-prism. A unity magnification IR optics (f/2) images the central 1.9×1.9 mm^2 area of the irradiated site onto an InSb focal-plane array (FPA) detector (liquid nitrogen cooled) of the IR camera (Galileo, Raytheon, Dallas, TX). Because μ_{IR} of skin varies by two orders of magnitude within the commonly utilized 3–5 μm detection band of the InSb detector, a custom filter narrows the acquisition band to 4.5–5.0 μm, whereby the effective value $\mu_{IR} = 26.5$ mm^{-1} was found to adequately represent optical properties of human skin.[21] A fixed aperture enables accurate positioning of the PWS test site in the object plane of the IR camera optics (see Fig. 1).

A digital delay generator was used to synchronize the pulsed laser emission and IR camera acquisition. By using a 64×64 subset of the FPA elements, the signal acquisition rate was 700 frames per second (at 0.9 ms integration time for each frame). The acquired data were digitized with a 12-bit A/D converter and stored in personal computer's memory. Finally, the PPTR signals $\Delta S(t)$ were computed by calibrating the system response using a computer-controlled blackbody (BB701, Omega Engineering, Stamford, CT), averaging laterally across the FPA, and subtracting the background signal level. Only one laser pulse needs to be applied for each PPTR measurement. However, in view of the severe ill-posednes of the ensuing mathematical analysis, each presented signal represents an average of three experimental recordings, acquired on the exact same skin site and under the same conditions, in order to reduce the signal-to-noise ratio.

The initial temperature profiles $\Delta T(z,0)$ were reconstructed by solving the inverse problem of heat diffusion and blackbody emission. We applied a conjugate-gradient iterative algorithm with a non-negativity constraint, and regularized by early termination. Such approach, combined with the so-called "L-curve" technique to determine the degree of regularization, has been shown to offer a good combination of speed and performance.[15] The presented examples, involving signal vectors with 950 elements and 64–100 unknown temperature values, required a couple of seconds CPU time on a 64-bit workstation (Sparc II, Sun Microsystems).

3. RESULTS

Figure 3a presents the arithmetic mean of three PPTR signals acquired from PWS on volunteer patient's hand (site A) after pulsed irradiation with the Tandem laser. Figure 3b shows a few characteristic temperature profiles $\Delta T(z,t=0)$, reconstructed from the signal in Figure 3a. The presented profiles include an under-iterated ($n = 5$; dashed line), representative ($n = 7$; heavy solid line), and perhaps over-iterated solution ($n = 10$; lighter solid line). The optimal iteration number is indicated by the "knee" in the corresponding L-curve (Fig. 3c), representing a log-log plot of the quadratic norm of the "image" (i.e., reconstructed temperature profile) against the norm of the residual (i.e., difference between the PPTR signal predicted from current solution and the experimental one).

Similarly, Figure 4 presents the averaged PPTR signal and the reconstructed temperature profiles for PWS on the same patient's forearm (site B), after pulsed irradiation with the same laser (Figs. 4a and 4b, respectively). Temperature profiles $\Delta T(z,t=0)$ presented in Figure 4b include under-iterated ($n = 5$; dashed line), representative ($n = 8$; heavy solid line), and pehaps over-iterated solution ($n = 10$; lighter solid line), according to L-curve analysis.

For the purposes of comparison, we present also temperature profiles induced in the same PWS sites A and B by pulsed irradiation with a KTP laser ($\lambda = 532$ nm, $H_0 = 1.8$ J/cm^2 - Figs. 5a and 5b, respectively). In these examples, convergence of the iterative image reconstruction is much better than that observed in Figures 3b and 4b.

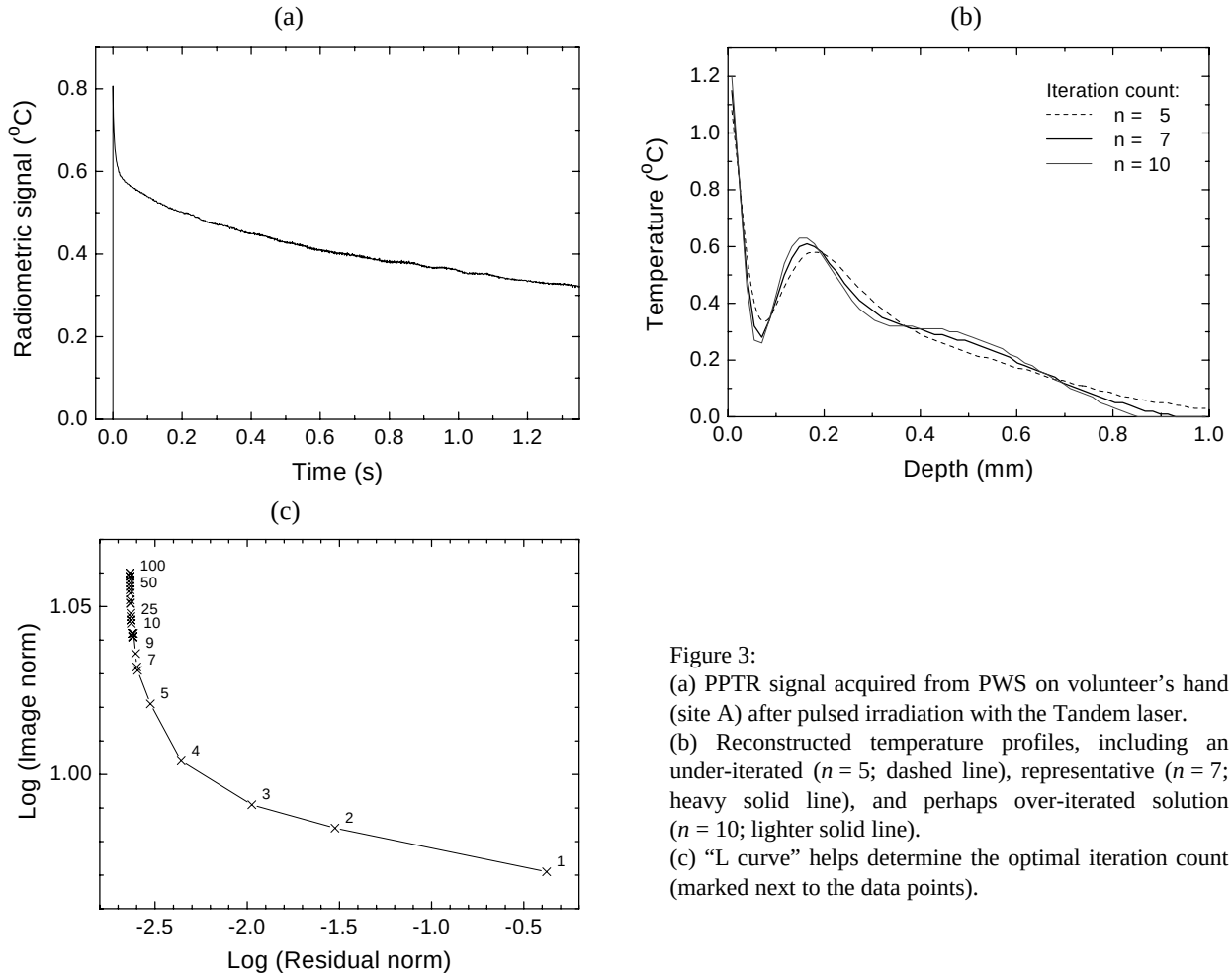

Figure 3:
(a) PPTR signal acquired from PWS on volunteer's hand (site A) after pulsed irradiation with the Tandem laser.
(b) Reconstructed temperature profiles, including an under-iterated (n = 5; dashed line), representative (n = 7; heavy solid line), and perhaps over-iterated solution (n = 10; lighter solid line).
(c) "L curve" helps determine the optimal iteration count (marked next to the data points).

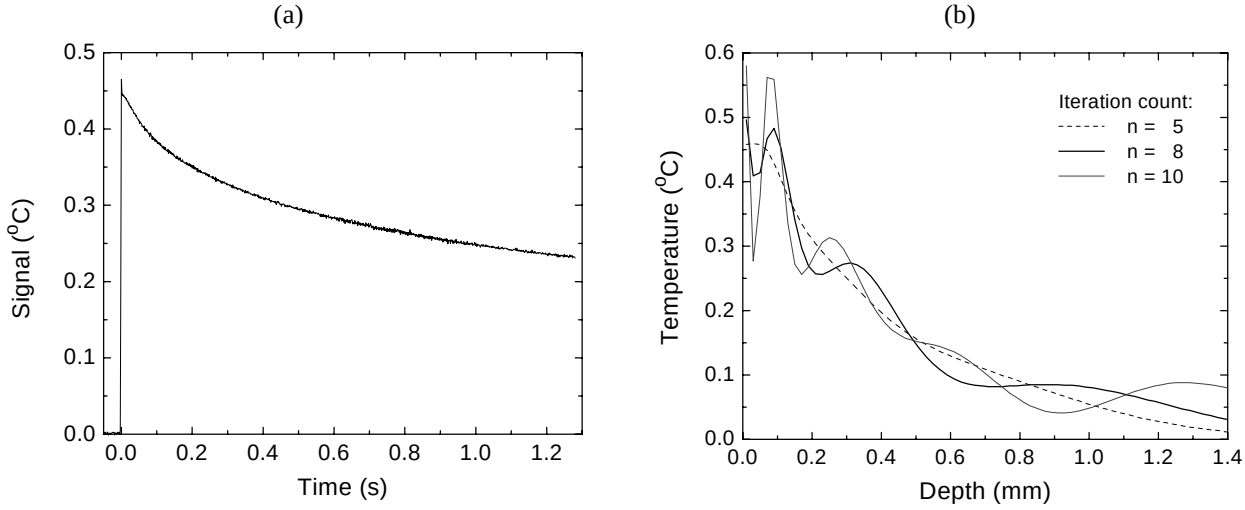

Figure 4: (a) PPTR signal acquired from PWS on patient's forearm (site B) after pulsed irradiation with the Tandem laser. (b) Reconstructed temperature profiles include under-iterated (dashed line), representative (heavy solid line), and perhaps over-iterated solutions (lighter solid line).

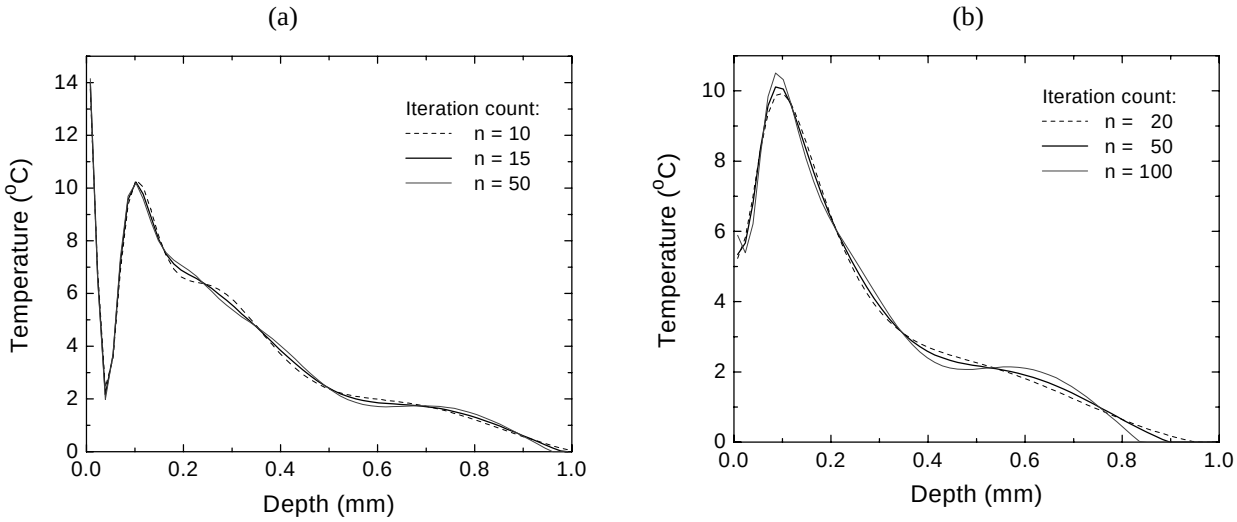

Figure 5: Temperature profiles induced in PWS sites A (a) and B (b) by pulsed irradiation with a KTP laser (λ = 532 nm, radiant exposure H_0 = 1.8 J/cm^2).

4. DISCUSSION

From simple calorimetric reasoning, it is evident that the area under the reconstructed temperature profile is proportional to surface density of the deposited energy, converted to heat (ε):

$$\varepsilon = \frac{E_{deposited}}{S} = \rho\, c \int_0^\infty \Delta T(z)\, dz\,. \qquad (3)$$

From known thermal properties of human dermis (mass density ρ = 1200 kg/m^3 and specific heat capacity c = 3800 J/kgK),[22] we can compute ε (3) for both PWS sites and irradiation lasers under test. The results are compared with respective radiant exposures (H_0) in Table 1.

Table 1: Surface density of the deposited laser energy (ε) assessed from the presented PPTR results, compared with the corresponding radiant exposures (H_0). Ratio of the two quantities (η_{dep}) indicates the fraction of delivered radiant exposure, converted to heat in PWS skin.

Laser (wavelength)	Tandem (532 nm + 1064 nm)		KTP (532 nm)	
PWS test site	A	B	A	B
H_0 [J/cm^2]	0.31		1.81	
ε [J/cm^2]	0.12	0.10	1.63	1.44
η_{dep} [-]	0.39	0.32	0.90	0.79

The fraction of delivered radiant exposure deposited as heat in the profiled skin layer ($\eta_{dep} = \varepsilon / H_0$) is evidently smaller with the Tandem laser as compared to irradiation at 532 nm alone (i.e., KTP laser). With the latter, the "missing" energy amounts to 10% and 21% of the incident value (for sites A and B, respectively). These values correspond nicely to reflectivity of PWS in fair (Caucasian) skin at the 532 nm wavelength,[23] which is strongly absorbed in both blood hemoglobin and epidermal melanin.

Starting from these values, and assuming that 36% of the energy emitted by the Tandem laser is at 532 nm, we derive that only 5–11% of the incident energy at 1064 nm is deposited as heat within the characterized skin layer. While this result is very unreliable (due to inaccurate input values and computationally unstable formulas involved), and likely exaggerate, the indicated trend is however plausible. Both hemoglobin and melanin absorption coefficients decrease rapidly towards the near IR, and the reflectivity of fair skin can exceed 50% at λ = 800 nm.[23]

More specifically, from λ = 532 nm to 1064 nm, the melanin absorption drops by almost a factor of 10,[4] and hemoglobin absorption by even more (a factor of 100–250, assuming 80% oxygenation level). This leads not only to strongly increased skin reflectivity, but also to large optical penetration depth at 1064 nm (on the order of mm), which is accentuated further by the lower value of the reduced scattering coefficient. Such effect is indicated by the non-negative, slowly decreasing temperature $\Delta T(z,t=0)$ at depth z = 1.4 mm in Tandem laser irradiation of PWS site B (Fig. 4b).

In each of the presented examples, the temperature profile was reconstructed in a z interval deep enough for the solution $\Delta T(z,t=0)$ to drop to 0 before its deep end. (In the example in Fig. 4b, e.g., the solution interval was 2.0 mm deep.) Accordingly, with integration in Eq. (3) extending over the whole solution interval, the presented ε values ideally encompass all deposited energy converted to heat. Nevertheless, amplitudes of the PPTR signal contributions from skin layers deeper than the heat diffusion length corresponding to the total signal acquisition time (t_a) decrease progressively. In the discussed experiments, $t_a \approx 1.3$ s, and heat deposition at depths beyond $z_D \sim 0.8$ mm may thereby not be reliably detected. We anticipate that this effect is more pronounced at low signal-to-noise ratios, such as occured in our Tandem measurements due to the very low radiant exposure. Until further evidence is obtained, we thereby allow that the unexpectedly low ratios η_{dep} assessed with the Tandem laser may be in part due to energy deposition at depths out of reach of PPTR profiling, in addition to the high skin reflectivity at 1064 nm.

In order to allow an objective comparison of the thermal effect of the two lasers, we present in Figure 6 temperature profiles upon pulsed irradiation of PWS test site A with the Tandem and KTP laser, normalized to a uniform radiant exposure of H_0 = 1 J/cm^2 (Figs. 6a and 6b, respectively). The plotted lines and error bars represent, respectively, the mean value and standard deviation of the temperature at each depth, as computed from a few near-optimal iterative solutions (Fig. 6a: n = 5-10; Fig. 6b: n = 10-50). Key characteristics of such normalized temperature profiles are collected in Table 2 (for both PWS test sites): superficial temperature value (T_1), subsurface temperature peak (T_2) and the depth of the latter (z_2).

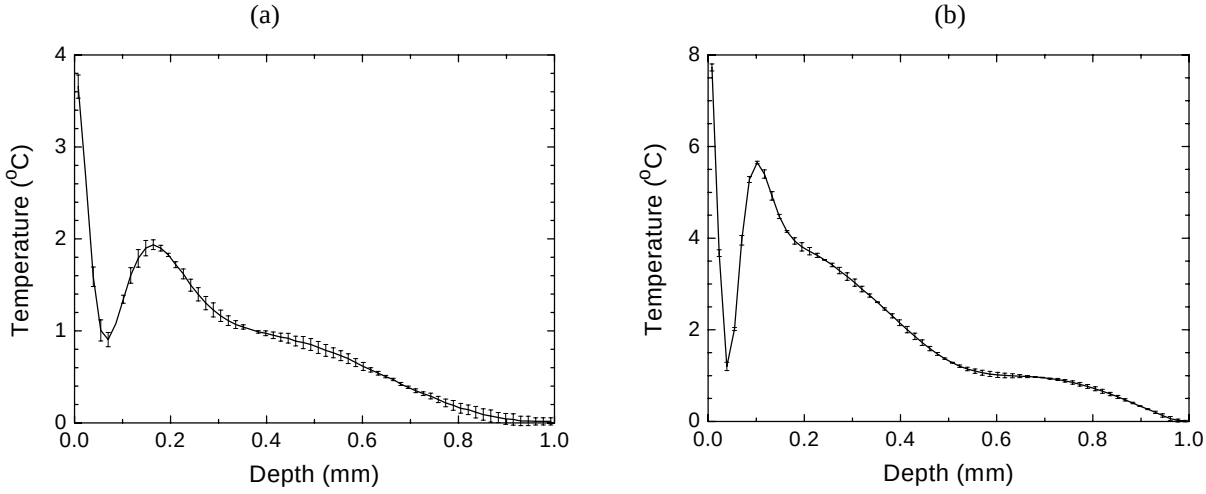

Figure 6: Temperature profiles in PWS (site A) immediately after pulsed irradiation with the Tandem (a), and KTP laser (b), at a hypothetical radiant exposure of H_0 = 1 J/cm^2. The solid lines and error bars represent, respectively, the mean value and standard deviation of the temperature at each depth, as computed from e few near-optimal iterative solutions: n = 5-10 (a); n = 10-50 (b).

Table 2: Key characteristics of temperature profiles induced in PWS sites A and B with a hypothetical radiant exposure of H_0 = 1 J/cm^2: superficial temperature value (T_1), subsurface temperature peak (T_2) and its depth (z_2).

Laser (wavelength)	Tandem (532 nm + 1064 nm)		KTP (532 nm)		Tandem, relative to KTP	
PWS site	A	B	A	B	A	B
T_1 [°C]	3.7	1.6	7.7	2.9	0.48	0.54
T_2 [°C]	1.9	1.5	5.6	5.6	0.34	0.27
z_2 [μm]	164 ± 8	90 ± 10	102 ± 8	94 ± 8	-	-

As seen in last two columns of Table 2, the ratio of the superficial temperature rise (T_1) obtained with the Tandem laser relative to KTP at the same radiant exposure is ~0.5. Doubling the radiant exposure customarily used with KTP lasers thereby appears appropriate in application of the Tandem laser system, as far as the amount of epidermal heating is concerned. Because the ratio of the corresponding T_2 values is significantly smaller than 0.5, one might conclude that the resulting vascular heating would be inferior to that obtained with a KTP laser at the original radiant exposure. However, such reasoning would be premature for several reasons:

First, the observed subsurface temperature peaks are quite superficial; most of the z_2 values in Table 2 fall within the range of typical basal layer depths (60–120 μm). It is very likely that these peaks do not arise exclusively from hemoglobin absorption, and so the T_2 values may not reflect the amount of induced vascular heating. In support of this claim, we present in Figure 7 the temperature profile in PWS site A, induced by pulsed irradiation with a pulsed dye laser (PDL) at 585 nm (ScleroPlus by Candela, Wayland, MA; pulse duration t_p = 1.5 ms, radiant exposure H_0 = 4.3 J/cm^2). The profile in Figure 7a features a superficial temperature of 17 °C, and a subsurface peak of 20 °C at z_2 = 88 ± 9 μm (n = 10). On the same PWS site, we have also performed so-called dual-wavelength excitation (DWE) PPTR profiling.[24,25] This technique allows separation of the epidermal and vascular components based on spectral differences between the melanin and hemoglobin at 585 and 600 nm, enabling more accurate and reliabile temperature profile reconstruction, in particular in shallow PWS. The result, presented in Fig. 7b, reveals markedly different amplitude (12 °C) and location of the peak PWS temperature (166 ± 9 μm) from the above values (heavy solid line). As is also evident from Figure 7b, the temperature peak at $z \leq 100$ μm arises as the sum of the melanin- and hemoglobin-contributed temperature profiles near the basal layer (lighter solid line). Judging by the close resemblance with the results in Figures 5a, 3b, etc., this effect is likely present in most of the above presented temperature profiles. (An exception might be the result in Figure 3b with z_2 = 164 μm, in accordance with the fact that the 1064 nm radiation is only minimally absorbed in the epidermal melanin.) Consequently, we have to conclude that the extracted T_2 values do not reflect reliably the induced heating of PWS.

Second, as Figure 7 also demonstrates, the surface temperature value (T_1) is often not reconstructed reliably in customary (i.e., single-wavelength) PPTR profiling of such relatively complex profiles. This is indicated also by the poor convergence in that part of the solution in Fig. 7a – in contrast with the DWE analysis, where reconstructions of the epidermal and PWS profiles are remarkably convergent and robust.[21,24,25] Although the DWE technique is still in process of optimization and rigorous testing,[25,26] it is safe to conclude that the maximal permissible light dose for the Tandem laser can not be reliably determined from the T_1 values in Table 2.

Nevertheless, note that the temperature rise at the basal layer, the most important epidermal structure – and the one that will be least protected by dynamic cooling – limits the maximal permissible radiant exposure in a therapeutic application. Thereby, inasmuch as the presented results represent the actual skin temperature profiles, the subsurface peak values (T_2 in Table 2), which are incidentally near the basal layer depth, determine the maximal radiant exposure. From such reasoning, three to four times higher radiant exposures might be safely applied with the Tandem laser, as compared to the customary KTP lasers (at the same pulse duration).

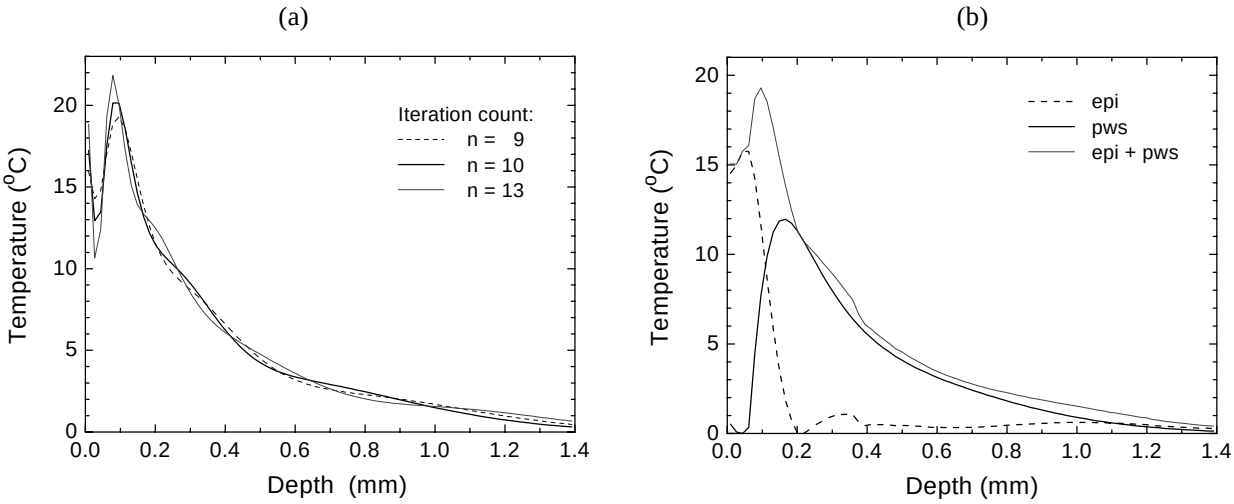

Figure 7: (a) Temperature profile in PWS site A after pulsed irradiation with a pulsed dye laser at 585 nm (H_0 = 4.3 J/cm^2; see text for details). (b) Epidermal (dashed line; n = 100) and vascular (heavy solid line; n = 100) contribution to the temperature profile, as determined by PPTR profiling with dual-wavelength excitation (λ = 585 and 600 nm). The lighter solid line is their sum, to be compared with the profiles in (a).

This factor correlates well with the ratio of the total vs. 532 nm emission from this laser (nominally 2.8), and the fact that the melanin absorption at 1064 nm is approximately 10 times lower than at 532 nm. In fact, from these two values alone, maximal permissible radiant exposures for the Tandem laser would scale by a factor of 2.4 higher than those for a comparable KTP laser. If 6–8 J/cm^2 is considered as a conservative estimate of the latter, radiant exposures around 20 J/cm^2, and accordingly higher with dynamic cooling, should be safe to apply with the Tandem laser. The ~12 J/cm^2 contribution at 1064 nm does certainly not present a medical hazard even if sizable portion of this radiation penetrates deeply into the skin, as several times higher radiant exposures are used routinely in Nd:YAG treatments of unwanted hair and vascular lesions.

Finally, while the above discussion was based on optical properties of native oxy- and deoxy-hemoglobin, chemical transformations during laser irradiation at 532 nm (tentatively to met-hemoglobin) were recently reported and studied by Barton et al.[27] From their data, first sings of transformation begin after deposition of ~3–5 J/cm^2 (delivered over 3–5 ms). Since radiant exposures in our measurements with Tandem and KTP lasers were significantly lower, we believe that the above mentioned effects can be disregarded in analysis of the presented data. However, such effects may play an important role in applications of the Tandem laser at therapeutic dosages as suggested above.

5. CONCLUSIONS

Pulsed photothermal radiometry is a viable tool for determination of temperature profiles induced in PWS in vivo with different laser systems. First measurements with the dual-wavelength laser system “Tandem” (emitting at 532 and 1064 nm simultaneously) suggest that 2.5–3 times higher radiant exposures may be applied with this laser than with a customary KTP laser (532 nm only) at similar pulse duration. A significant amount of deep heating (at the 0.5–1.5 mm depths) was observed in one measurement with the Tandem laser, which may be very promising for treatment of deeper and larger vessels, and perhaps even hair removal. More detailed analysis and/or further measurements, perhaps involving DWE, will be necessary to extract quantitative information, since the blood induced temperature profiles and epidermal heating were overlapping in both PWS sites under test, effectively preventing determination of the individual contributions to dermal heating.

ACKNOWLEDGEMENTS

The authors thank Fotona d.d. (Ljubljana, Slovenia) for the loan of the Tandem laser system. The work was supported by the Slovenian Ministry of Science and Technology (BM), Arnold and Mabel Beckman Fellows Program (BC), and research grants from the National Institutes of Health (NIH; AR-43419 and GM-62177 to JSN). Institutional support from the Office of Naval Research, NIH, and the Beckman Laser Institute and Medical Clinic Endowment is also acknowledged.

REFERENCES

1. S. H. Barsky, S. Rosen, D. E. Geer, and J. M. Noe, "The nature and evolution of port wine stains: a computer-assisted study," *J. Invest. Dermatol.* **74**, pp. 154-157, 1980.
2. J. S. Nelson, T. E. Milner, B. Anvari, B. S. Tanenbaum, S. Kimel, L. O. Svaasand, and S. L. Jacques, "Dynamic epidermal cooling during pulsed laser treatment of port-wine stain. A new methodology with preliminary clinical evaluation," *Arch. Dermatol.* **131**, pp. 695-700, 1995.
3. J. S. Nelson, B. Majaron, and K. M. Kelly, "Active skin cooling in conjunction with laser dermatologic surgery," *Semin. Cutan. Med. Surg.* **19**, pp. 253-266, 2000.
4. I. V. Meglinsky and S. J. Matcher, "The determination of absorption coefficient of skin melanin in visible and NIR spectral region," in: Lasers in Surgery: Advanced Characterization, Theraputics, and Systems X, *Proc. SPIE* **3907**, pp. 143-150, Bellingham, WA, 2000.
5. N. S. Sadick, "Long-term results with a multiple synchronized-pulse 1064 nm Nd:YAG laser for the treatment of leg venulectasias and reticular veins," *Dermatol. Surg.* **27**, pp. 365-369, 2001.
6. P. Kaudewitz, W. Klövekorn, and W. Rother, "Treatment of Leg Vein Telangiectases: 1-Year Results With a New 940 nm Diode Laser," *Dermatol. Surg.* **28**, p.1031, 2002.
7. N. E. Omura, J. S. Dover, K. A. Arndt, A. N. Kauvar, "Treatment of reticular leg veins with a 1064 nm long-pulsed Nd:YAG laser," *J. Am. Acad. Dermatol.* **48**, pp. 76-81, 2003.
8. A. C. Tam and B. Sullivan, "Remote sensing applications of pulsed photothermal radiometry," *Appl. Phys. Lett.* **43**, pp. 333-335, 1983.
9. R. E. Imhof, D. J. S. Birch , F. R. Thornley, J. R. Gilchrist, and T. A. Strivens, "Optothermal transient emission radiometry," *J. Phys. E: Sci. Instrum.* **17**, pp. 521-525, 1984.
10. F. H. Long, R. R. Anderson, and T. F. Deutch, "Pulsed photothermal radiometry for depth profiling of layered media," *Appl. Phys. Lett.* **51**, pp. 2076-2078, 1987.
11. R. M. S. Bindra, R. E. Imhof, and G. M. Eccleston, "In vivo opto-thermal measurement of epidermal thickness," *J. De Physique IV* **C7**, pp. 445-448, 1994.
12. I. A. Vitkin, B. C. Wilson, and R. R. Anderson, "Analysis of layered scattering materials by pulsed photothermal radiometry – application to photon propagation in tissue," *Appl. Opt.* **34**, pp. 2973-2982, 1995.
13. S. A. Prahl, I. A. Vitkin, U. Bruggeman, B. C. Wilson, and R. R. Anderson, "Determination of optical properties of turbid media using pulsed photothermal radiometry," *Phys. Med. Biol.* **37**, pp. 1203-1217, 1992.
14. S. L. Jacques, J. S. Nelson, W. H. Wright, and T. E. Milner, "Pulsed photothermal radiometry of port-wine-stain lesions," *Appl. Opt.* **32**, pp. 2439-2446, 1993.
15. T. E. Milner, D. M. Goodman, B. S. Tanenbaum, and J. S. Nelson, "Depth profiling of laser-heated chromophores in biological tissues by pulsed photothermal radiometry," *J. Opt. Soc. Am.* **A 12**, pp. 1479-1488, 1995.
16. T. E. Milner, D. J. Smithies, D. M. Goodman, A. Lau, and J. S. Nelson, "Depth determination of chromophores in human skin by pulsed photothermal radiometry," *Appl. Opt.* **35**, pp. 3379-3385, 1996.
17. S. A. Telenkov, D. J. Smithies, D. M. Goodman, B. S. Tanenbaum, J. S. Nelson, and T. E. Milner, "Infrared imaging of *in vivo* microvasculature following pulsed laser irradiation," *J. Biomed. Opt.* **3**, pp. 391-395, 1998.
18. B. Majaron, T. E. Milner, and J. S. Nelson, "Pulsed photothermal imaging of port-wine stain birthmarks using two laser wavelengths," *Lasers Surg. Med*. **sup 14**, p. 8, 2002.

19. B. Majaron, T. E. Milner, and J.S. Nelson, “Optical characterization of port wine stain lesions for individual optimization of laser therapy,” *J. Cosmetic & Laser Ther.* **4**, p. 53, 2002.
20. S. A. Prahl, “Pulsed photothermal radiometry of inhomogeneous tissue,” in: *Progress in Photothermal and Photoacoustic Science and Technology Series: Life and Earth Sciences*, vol. 3, A. Mandelis and P. Hess, eds. (SPIE, Bellingham, 1997).
21. B. Majaron, W. Verkruysse, B. S. Tanenbaum, T. E. Milner, and J. S. Nelson, “Spectral variation of infrared absorption coefficient in pulsed photothermal profiling of biological samples,” *Phys. Med. Biol.* **47**, pp. 1929-1946, 2002.
22. F. A. Duck, *Physical Properties of Tissue*, Academic Press, London, 1990, chap. 2.
23. L. O. Svaasand, L. T. Norvang, E. J. Fiskerstrand, E. K. S. Stopps, M. W. Berns, and J. S. Nelson, “Tissue parameters determining the visual appearance of normal skin and port-wine stains,” *Lasers Med. Science* **10**, pp. 55-65, 1995.
24. B. Majaron, W. Verkruysse, B. S. Tanenbaum, T. E. Milner, S. A. Telenkov, D. M. Goodman, and J. S. Nelson, “Combining two excitation wavelengths for pulsed photothermal profiling of hypervascular lesions in human skin,” *Phys. Med. Biol.* **45**, pp. 1913–1922, 2000.
25. B. Majaron, T. E. Milner, and J. S. Nelson, “Determination of parameter β for dual-wavelength pulsed photothermal profiling of human skin,” *Rev. Sci. Instrum.* **74**, pp. 387-389, 2003.
26. B. Choi, B. Majaron, and J.S. Nelson, “Theoretical evaluation of pulsed photothermal radiometry (PPTR) for depth profiling of port wine stain skin,” in: Lasers in Surgery: Advanced Characterization, Theraputics, and Systems XIII, *Proc. SPIE* **4949**, Bellingham, WA, 2003 – in press.
27. J. K. Barton, G. Frangineas, H. Pummer, J. F. Black, “Cooperative phenomena in two-pulse, two-color laser photocoagulation of cutaneous blood vessels,” *Photochem. Photobiol.* **73**, pp. 642-650, 2001.